Development and Characterization of Gadolinium-Doped Hydroxyapatite to Enhance Biocompatibility in Biomedical Applications

Swadhi Radhakrishnan*, Gayathri Krishnan, Anitha Rexalin Devaraj, Rajesh Krishnan, Anandan Kasinatha

Department of Physics, Academy of Maritime Education and Training, Chennai, India

Abstract

The synthesis and characterization of gadolinium-doped brucinium hydroxyapatite (Gd-BHAP) have garnered significant attention for their potential applications in bone regeneration and dentistry. Hydroxyapatite (HAP) closely resembles the mineral phase of bone, exhibiting biocompatibility, biodegradability, and bioactivity. Hence, this study aims to synthesize and characterize Gd-BHAP to evaluate its potential for enhancing biocompatibility and effectiveness in bone regeneration applications. Gd-BHAP was synthesized via a hydrothermal method using calcium nitrate tetrahydrate and diammonium hydrogen phosphate as precursors, maintaining a calcium-to-phosphate molar ratio of 1:6. Dual dopants, brucine (1%) and gadolinium (+0.5%, 1%, and 2% concentrations), were incorporated, with the pH adjusted to 9. Characterization was performed using XRD, SEM, DLS, FTIR, Fluorescence and UV-Vis spectroscopy. The cytotoxicity of Gd-BHAP was evaluated on Vero cells using the MTT assay across varying concentrations (25–200 µg/mL). Results indicated that the characterization techniques confirmed the successful synthesis of Gd-BHAP, demonstrating rod-shaped morphology and sizes ranging from 70 to 121 nm. FTIR analysis revealed typical absorption bands of hydroxyapatite, while XRD patterns matched known standards for HA, indicating a hexagonal phase. Cytotoxicity results showed a concentration-dependent decrease in Vero cell viability, with 84% viability at 25 µg/mL, decreasing to 73% at 200 µg/mL, indicating acceptable biocompatibility for potential biomedical applications. In conclusion, the synthesized gadolinium-doped brucinium hydroxyapatite exhibits promising characteristics for biomedical applications, particularly in bone regeneration. While higher concentrations may reduce cell viability, the material demonstrates significant biocompatibility, positioning it as a suitable candidate for tissue engineering.

Keywords: Biocompatibility, Biocompatibility, Biomedical, Gadolinium-Doped Brucinium Hydroxyapatite, Hydroxyapatite.

Introduction

The development of nanosized carriers for drug delivery to tumour sites is one of the most active fields in nanomedicine [1]. Constructing drug carriers with excellent biocompatibility is crucial for the clinical translation of these nanosystems [2, 3]. In recent years, hydroxyapatite (HAP), a calcium phosphate bioceramic, has gained attention as a building block for nanosized drug carriers due to its bioactivity, non-toxic nature, and non-inflammatory properties [4, 5, 6]. HAP is well-known for its suitability in bone tissue regeneration [7], owing to its biocompatibility [8, 9], good mechanical properties [10], osteoconductivity [11, 12], and ability to form chemical bonds with bone tissue [13, 14]. This ceramic has been utilized for treating bone defects [10, 15] however, the mechanical strength of most hydroxyapatite scaffolds

fabricated to date is lower than that of healthy bone [16]. Despite this, HAP is favourable compared to other naturally derived biomaterials, and ion doping has been extensively investigated to improve its mechanical properties [13, 17]. Alternatives that offer superior load-bearing and mechanical properties, such as metals and ceramics, are often inert, not biocompatible, and unsupportive of isomorphic tissue replacement [18]. Although HAP shows promise, its biological activity remains limited [19]. A single material often cannot meet the requirements for effective bone repair, so combining HAP with biologically active metabolites or drugs through doping can enhance its biomedical properties for therapeutic applications [20, 21].

Various dopants can be easily incorporated into the lattice of HAP, bestowing HAP nanoparticles with desired functionalities for medical applications, including bioimaging [22, 23]. Recent advances in preparing nanosized HAP with customized surface characteristics and colloidal stability have opened new perspectives for their use in non-bone-related applications [24]. HAP's highly flexible structure can accommodate foreign ions, inducing changes in its physicochemical properties [25]. It has been observed that HAP nanoparticles can exhibit a range of abilities that pure HAP does not possess, including photocatalytic, luminescent, and magnetic properties through various doping methods [26, 27]. Currently, gadolinium is the only dopant approved for human use as a T1 contrast agent [28, 29]. However, gadolinium can induce nephrogenic systemic fibrosis (NSF), which presents as cutaneous fibrosing impairment within days or months following injection and may lead to severe renal failure in the future [30].

Based on the rationale provided, gadolinium-doped brucinium hydroxyapatite may serve as an alternative biomaterial for enhancing biocompatibility in various applications due to its functional properties. Therefore, this research aims to synthesize gadolinium-doped brucinium hydroxyapatite and investigate its characterization, functional properties, and biological activity.

Materials and Methods

Synthesis of Gadolinium-Doped Brucinium Hydroxyapatite via Hydrothermal Method

Calcium and phosphate are the main components of hydroxyapatite. To synthesize hydroxyapatite, calcium nitrate tetrahydrate Ca $(NO_3)_2.4H_2O$ (Brand: Merck >98.0%) and and diammonium hydrogen phosphate $(NH_4)_2 HPO_4$ were used as precursors. Calcium and phosphate were taken in a molar ratio of 1:6. Dual dopants, brucine $(C_{23}H_{26}N_2O_4)$ (Loba, 99%) and gadolinium (III) nitrate hexahydrate $(Gd (HO_3)_3.6H_2O)$ were added. The pH was maintained at 9 by adding liquid ammonium (NH_4OH). The composition of brucine was optimized at 1%, while the doping percentage of gadolinium was varied at 0.5%, 1%, and 2%. The synthesis was carried out using a hydrothermal method at a temperature of 180°C for 24 hours. Gd-doped brucinium hydroxyapatite was obtained after centrifugation and subsequently dried at 100°C.

Characterization of Gadolinium-Doped Brucinium Hydroxyapatite

The synthesized Gadolinium-Doped Brucinium Hydroxyapatite was characterized using various instrumentation techniques, including X-ray Diffraction (XRD) (Davinci X-ray diffractometer with Cu K_α (λ = 1.540 Å)), Scanning Electron Microscopy (SEM) (Carl Zeiss, Model: EVO 18), Dynamic Light Scattering (DLS) (Nano Plus with a 70mW diode laser (660 nm)), Fourier Transform Infrared Spectroscopy (FTIR) (Thorlabs LM74S2 Driver, Thorlabs Laser Diode Control LDC2000-2A).

Cytotoxicity Analysis of Gadolinium-Doped Brucinium Hydroxyapatite

The cytotoxic properties of Gadolinium-Doped Brucinium Hydroxyapatite were assessed using the MTT assay on Vero cell lines in vitro. After removing the culture medium, the Vero cells were subcultured in DMEM supplemented with 10% FCS. The cells were homogenized in 25 mL of DMEM by gently pipetting the medium to suspend the cells. A 24-well culture plate was filled with 1 mL of the homogenized cell suspension and treated with varying concentrations of the sample (50–250 µg/mL). The plate was placed in a humidified CO_2 incubator (5%) and maintained at 37°C. After a 48-hour incubation period, a cytotoxicity assay was performed on the Vero cells, which were 80% confluent as observed under an inverted microscope. The MTT assay used 3-(4,5-dimethylthiazol-2-yl)-2,5-diphenyltetrazolium bromide (MTT) at different sample concentrations (25, 50, 100, and 200 µg/mL). Mitochondrial enzymes in viable cells reduced MTT to a measurable purple formazan product, which was inversely correlated with cytotoxicity and directly correlated with the number of viable cells. After incubation, 5 µg/mL of MTT was added to the wells, and the plate was incubated at room temperature for 3 hours. The formazan crystals were then dissolved by adding 100 µL of DMSO after the contents of the wells were removed by pipetting. Absorbance was measured using a Readwell Touch microplate reader at 570 nm.

Results and Discussion

The application of synthesized biomaterials in the fields of bone regeneration and dentistry has garnered significant attention, with notable efforts made to synthesize biomaterials through various routes using different sources. Hydroxyapatite (HAP), in particular, due to its close chemical similarity to the mineral phase of bone, is ranked highly as one of the most promising biomaterials. It is well-known for its excellent biocompatibility, biodegradability, bioactivity, non-toxicity, and non-inflammatory properties, which make it suitable for a wide range of biomedical applications, such as bone cavity filling material, drug delivery systems, bone substitutes, implant components, coatings on implants, cancer hyperthermia treatment, dental materials, and more. The ability of HAP to promote bone growth within bone tissue makes it an excellent candidate for use as a hard tissue implant material. Additionally, apart from biomedical applications, many other remarkable and diverse uses of HAP, especially when doped with gadolinium, have been reported. This study focuses on the synthesis and characterization of gadolinium-doped brucinium hydroxyapatite, investigating its functional properties and biological activity.

Characterization of Gadolinium-Doped Brucinium Hydroxyapatite

Hydroxyapatite closely resembles natural bone in composition, and its structure makes it ideal for biomedical applications. Characterization is essential to determine how different synthesis methods affect the properties of HAP nanoparticles, which are used in bone regeneration, dental applications, and drug delivery. In this study, gadolinium-doped brucinium hydroxyapatite was characterized using FTIR, XRD, SEM and DLS.

FTIR Analysis of Gadolinium-Doped Brucinium Hydroxyapatite

FTIR analysis is commonly used to identify and characterize unknown materials and to detect additives after extraction from a polymer matrix. In this study, the FTIR analysis of gadolinium-doped brucinium hydroxyapatite revealed typical absorption bands of hydroxyapatite (Gd-BHAP). The functional group analysis for synthesized

hydroxyapatite (HAP) and gadolinium-doped brucinium hydroxyapatite (Gd-BHAP) was carried out in the range of 4000 cm^{-1} to 600 cm^{-1}, as shown in Figure -1. The characteristic peaks of HAP were observed at 500–650 cm^{-1}, 958 cm^{-1}, 1032 cm^{-1}, 1093 cm^{-1}, 1381 cm^{-1}, and 3400–3600 cm^{-1}.

The ν_2 and ν_4 bending vibrational modes of the phosphate group (PO_4^{3-}) were detected at 465 cm^{-1}, 560 cm^{-1}, and 603 cm^{-1}, while the peak at 958 cm^{-1} corresponds to the ν_1 stretching vibrational mode. The peaks at 1032 cm^{-1} and 1093 cm^{-1} represent the ν_3 stretching

vibrational modes of the phosphate group (PO_4^{3-}). The broad peak at 3416 cm^{-1} corresponds to the O-H stretching vibration due to the intermolecular hydrogen bonding of water. The peak at 3580 cm^{-1} is assigned to the stretching vibrational mode of the hydroxyl group (-OH), while the sharp peak at 1381 cm^{-1} and the shoulder peak at 1631 cm^{-1} represent the bending vibrational mode of hydroxyl groups (-OH) from water absorbed by HAP. The peak at 1712 cm^{-1} corresponds to the C=O stretching vibrational mode of HAP.
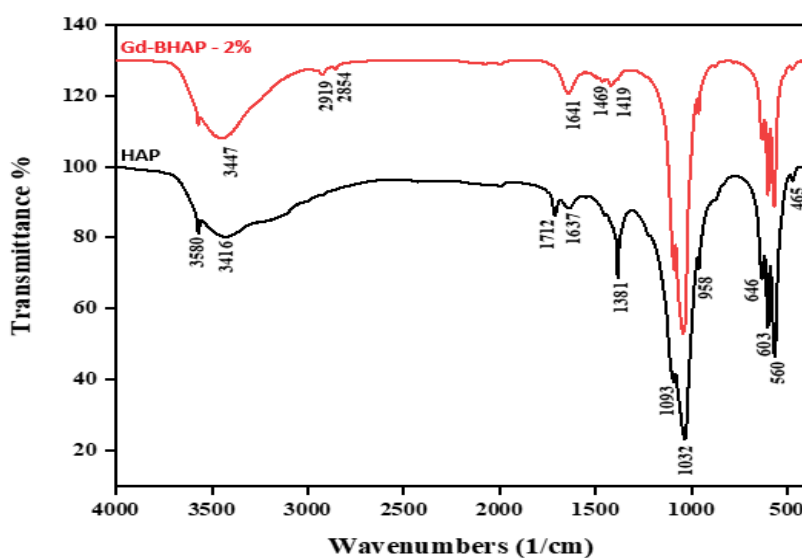

Figure 1. Fourier Transform Infrared Spectroscopy (FTIR) Analysis of Gadolinium-Doped Brucinium Hydroxyapatite

A slight shift with an intense peak at 3447 cm^{-1} indicates the N-H and N-O vibrational stretching due to the chemical interaction of brucine with HAP. The shift at 1641 cm^{-1} represents the bending vibrational changes of the hydroxyl group about brucine. When gadolinium was added as a dopant for use as a contrast agent, its effects were seen in the addition of two coupled peaks at 2919 cm^{-1} and 2854 cm^{-1}, corresponding to the C-H stretching vibrational modes. Additionally, the peaks at 1469 cm^{-1} and 1419 cm^{-1} correspond to the ν_3 stretching vibrational modes of the carbonate group (CO_3^{2-}) due to carbon-carbon interactions. Similar results have been reported

in other studies on hydroxyapatite [31, 32, 33, 34].

XRD Analysis of Gadolinium-Doped Brucinium Hydroxyapatite

X-ray diffraction (XRD) analysis of hydroxyapatite (HAP) is crucial for understanding the material's crystalline nature, stability, and interactions with different environments. XRD can also confirm the mineralogy of HAP, ensuring compliance with regulatory standards. The X-ray diffraction patterns of pure hydroxyapatite (HAP) and gadolinium-doped brucinium hydroxyapatite (Gd-BHAP) nanorods are shown in Figure 2. The diffraction pattern of synthesized HAP

exhibits prominent phase planes at (0, 0, 2), (2, 1, 1), (1, 1, 2), and (2, 0, 2), which correspond well with the Joint Committee on Powder Diffraction Standards (JCPDS) data (Ref: PDF# 72-566). The material was identified as having a hexagonal phase, with lattice parameters a = b = 9.4240 Å and c = 6.8790 Å.

A similar structure was observed for Gd-BHAP nanorods, as the minimal percentage of gadolinium dopant did not introduce any additional peaks or alter the phase composition, which remained the same as that of the parent hydroxyapatite material.
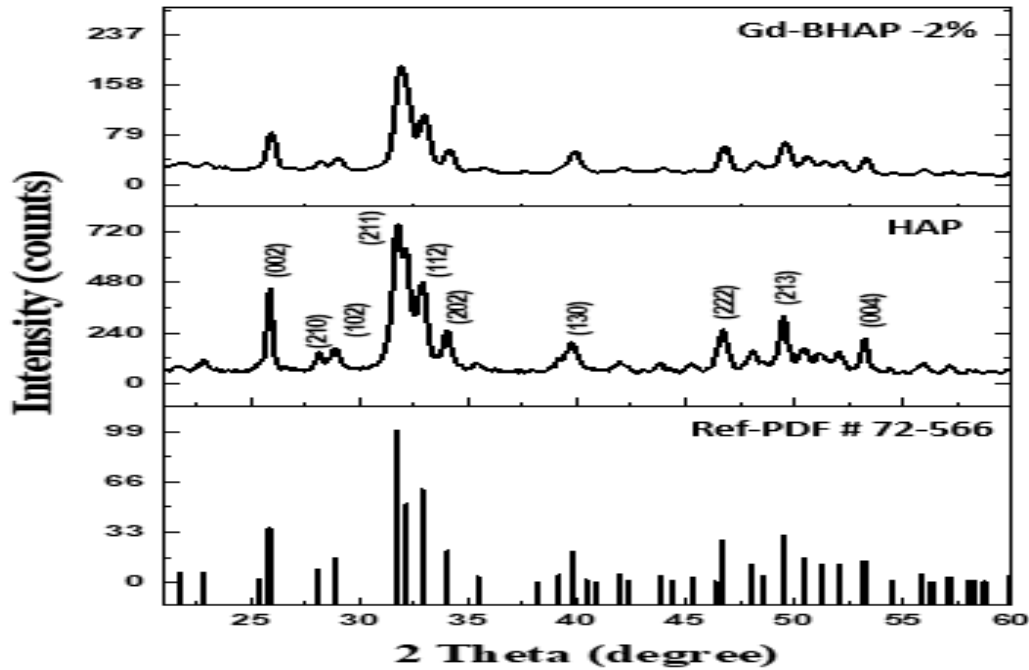

Figure-2. XRD Analysis of Gadolinium-Doped Brucinium Hydroxyapatite

The crystal size (D) was determined using Full Width at Half Maximum (FWHM) through a Gaussian fit. According to the Scherrer equation:

$$Crystalline\ Size(D) = \frac{0.9\lambda}{\beta\ cos\theta}.$$

Where λ = 1.5405 Å (wavelength of Cu-Kα radiation), β is the FWHM of the peaks, and θ is the Bragg diffraction angle. The crystalline size was found to be between 70 and 120 nm. Similarly, the crystalline size of HAP is 120 nm with luminescence properties [35]. The estimated average crystallite sizes are 10 nm for biological hydroxyapatite extracted from human mandible bone and 8 nm for carbonated hydroxyapatite [36].

SEM Analysis of Gadolinium-Doped Brucinium Hydroxyapatite

Scanning Electron Microscopy (SEM) analysis of hydroxyapatite (Gd-BHAP) is crucial as it provides insights into the particle shape, size, and agglomeration. In this study, the SEM images of the synthesized gadolinium-doped brucinium hydroxyapatite are shown in Figure -3. These images confirm the agglomerated nature of the sample and the rod-shaped morphology. Similarly, the agglomerated nature and rod-shaped morphology of nano-hydroxyapatite (n-HAP) were synthesized using the wet chemical technique [38]. Additionally, observed rod-like nano-hydroxyapatite integrated into the type I collagen matrix, demonstrating its potential use in 3D printing of bone scaffolds [39].
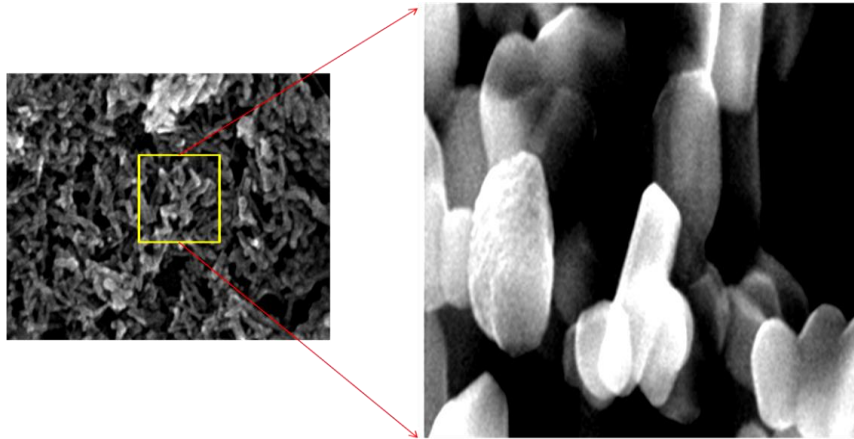
Figure -3. SEM Analysis of Gadolinium-Doped Brucinium Hydroxyapatite

DLS Analysis of Gadolinium-Doped Brucinium Hydroxyapatite

Dynamic Light Scattering (DLS) is a technique used to measure the average particle size and size distribution by dispersing the particles in a solution. This analytic method is noted for its speed, noninvasive nature, and sensitivity to nanoparticles. The scattering mechanism is based on the principle of Brownian motion, where smaller particles move faster and larger particles move more slowly. The translational diffusion coefficient (D) can be calculated from the speed of Brownian motion, which helps derive the hydrodynamic diameter (D_H).

The hydrodynamic diameter is calculated using the Stokes-Einstein equation:

$$Hydrodynamc\ Diameter\ (D_H) = \frac{K_B T}{3\pi\eta D}.$$

Where $K_B T$ is the Boltzmann constant, T is the temperature, and η is the dispersant viscosity. The average size of the synthesized Gd-BHAP particles ranged from 73 nm to 121 nm (Figure – 4). Based on this analysis, the Gadolinium-Doped Brucinium Hydroxyapatite shows potential for tissue engineering applications, particularly in scaffold development [40].
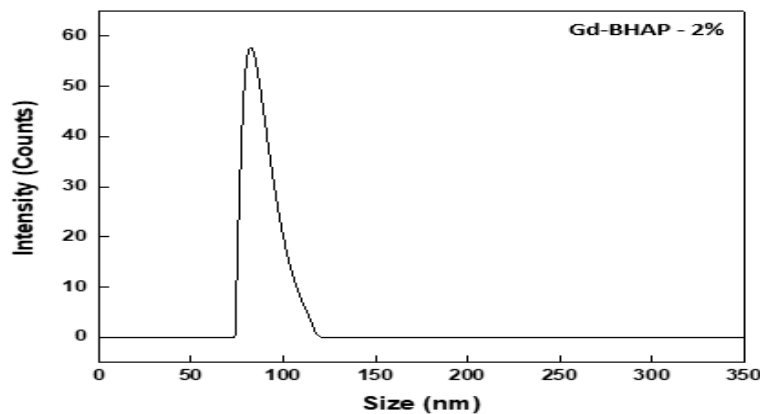

Figure -4. DLS Analysis of Gadolinium-Doped Brucinium Hydroxyapatite

Fluorescence Spectrum of Gadolinium-Doped Brucinium Hydroxyapatite

The fluorescence spectrum of hydroxyapatite (Gd-BHAP) can vary depending on the type of HAP and the conditions of excitation and measurement. Gadolinium typically exhibits emission within the wavelength range of 300 to 350 nm. However, the synthesized Gd-BHAP demonstrated a significant shift in its emission

profile, characterized by an increase in emission intensity. Furthermore, a distinct and prominent peak was observed within the 650 to 750 nm range, a feature strongly associated with gadolinium [40, 41]. The fluorescence spectra of both HAP and Gd-BHAP are shown in Figure (5). HAP, by itself, does not exhibit fluorescence properties, but previous literature highlights the fluorescence property induced by hydrothermal synthesis due to the existence of CO** radicals when the precursor material is introduced. Prior research has observed emission peaks around 400 nm to 460 nm (violet to blue) [42, 43].
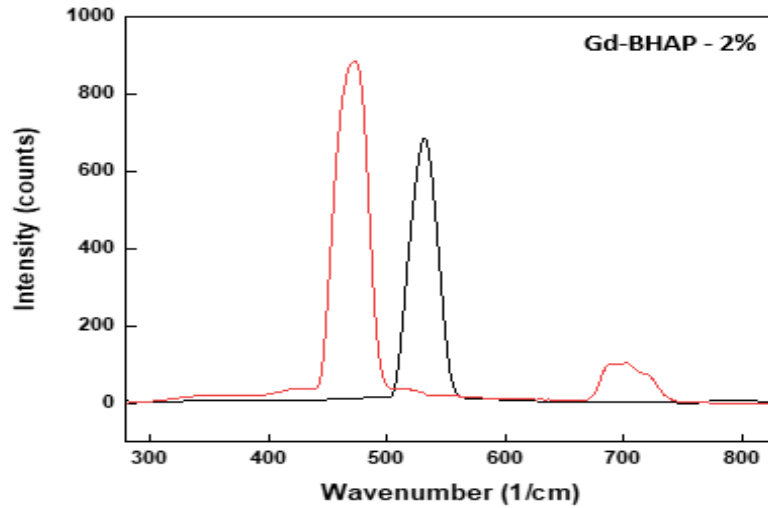

Figure -5. Fluorescence Spectrum of Gadolinium-Doped Brucinium Hydroxyapatite

UV-Vis Spectroscopy and the Tauc Plot of Gadolinium-Doped Brucinium Hydroxyapatite

UV-Vis spectroscopy and the Tauc plot are used together to determine the optical band gap. The Gadolinium-Doped Brucinium Hydroxyapatite exhibits a strong absorption peak in the ultraviolet region. The band gap of Gd-BHAP aligns with the calculated band gap of hydroxyapatite containing an oxygen vacancy structure, indicating that the phosphate group in HAP contains oxygen vacancies. However, the bandwidth of these composite materials allows for the generation of photogenerated electrons and holes when excited by visible light [44].
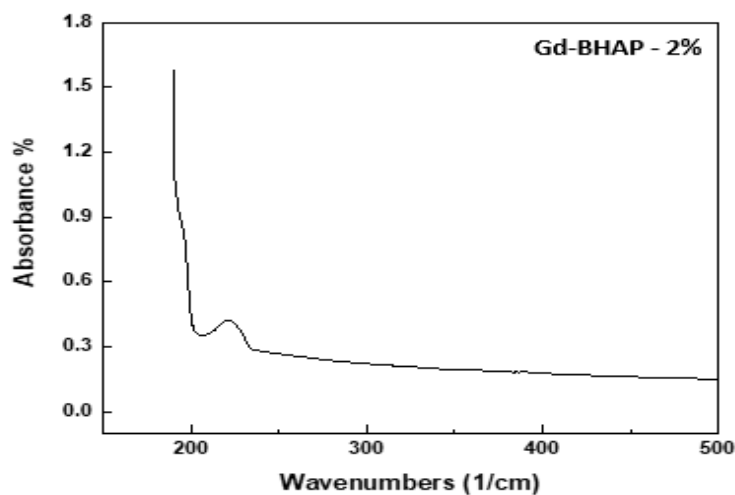

Figure -6. UV-Vis Spectroscopy Analysis of Gadolinium-Doped Brucinium Hydroxyapatite
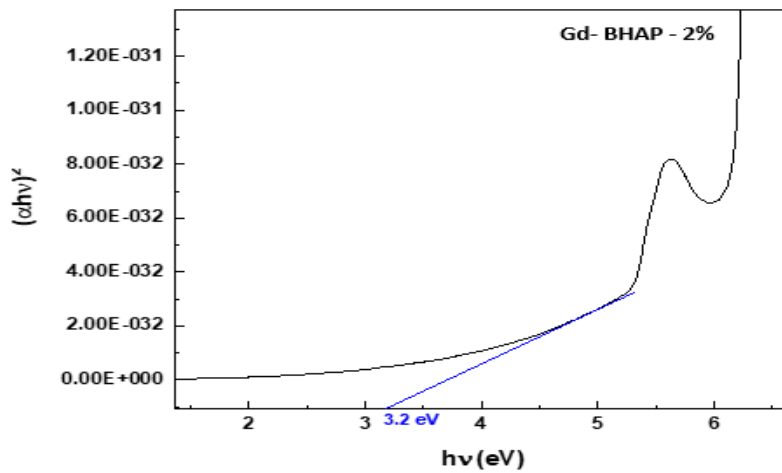
Figure -7. Tauc Plot of Gadolinium-Doped Brucinium Hydroxyapatite

Cytotoxicity Analysis of Gadolinium-Doped Brucinium Hydroxyapatite against Vero Cells

Cell viability can be assessed using the sensitive and dependable MTT assay. This test depends on the capacity of cellular mitochondrial dehydrogenase enzymes to convert the yellow, water-soluble substrate 3-(4,5-dimethylthiazol-2-yl)-2,5-diphenyl tetrazolium bromide (MTT) into the dark blue or purple, water-insoluble formazan product [45]. The amount of formazan generated is directly related to the number of cells in various cell lines. Previous literature evaluated in vitro cytotoxicity tests using Vero cells from the African green monkey [46]. These toxicity tests demonstrated that the evaluated composites are not toxic. The biomaterials exhibited good biocompatibility and no

evidence of cytotoxicity, making them good candidates for tissue graft engineering and bone regeneration [46]. The results of the cytotoxicity analysis indicated that Gadolinium-Doped Brucinium Hydroxyapatite has a concentration-dependent effect on Vero cell viability. At a concentration of 25 µg/mL, cell viability was 84%, which slightly decreased to 79% at 50 µg/mL. Further increases in concentration led to additional declines in viability, with 75% at 100 µg/mL and 73% at 200 µg/mL. These results suggest that while Gadolinium-Doped Brucinium Hydroxyapatite maintains relatively high cell viability at lower concentrations, higher concentrations may reduce viability, yet they still indicate acceptable biocompatibility for potential biomedical applications.
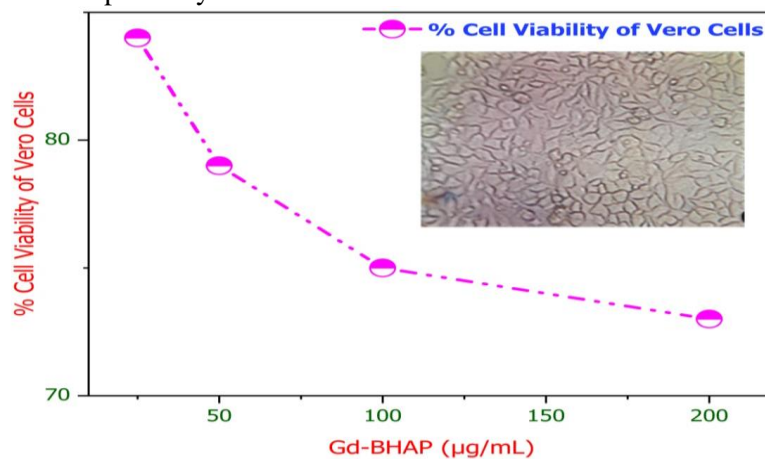

Figure 8. Cytotoxic Analysis of Gadolinium-Doped Brucinium Hydroxyapatite Against Vero Cells

Conclusion

In this study, we have successfully synthesized gadolinium-doped brucinium hydroxyapatite using a hydrothermal method with calcium nitrate tetrahydrate, diammonium hydrogen phosphate, brucine, and gadolinium nitrate. Characterization techniques such as FTIR, XRD, SEM, and DLS confirmed its structural and morphological properties. The synthesized hydroxyapatite demonstrated excellent biocompatibility, as shown by cytotoxicity tests on Vero cell lines using the MTT assay, indicating high cell viability at lower concentrations and a concentration-dependent cytotoxic effect at higher levels. Overall, this material shows promise for biomedical applications, particularly in tissue engineering and bone regeneration, providing valuable insights for advancing biomaterials in regenerative medicine.

References

[1]. Lara-Ochoa, S., Ortega-Lara, W., & Guerrero-Beltrán, C. E., 2021. Hydroxyapatite nanoparticles in drug delivery: physicochemistry and applications. *Pharmaceutics*, *13*(10), 1642.

[2]. Cheng, X., Wei, J., Ge, Q., Xing, D., Zhou, X., Qian, Y., & Jiang, G. 2021. The optimized drug delivery systems of treating cancer bone metastatic osteolysis with nanomaterials. *Drug Delivery*, *28*(1), 37-53.

[3]. De Lama-Odría, M. D. C., Del Valle, L. J., & Puiggalí, J. 2022. Hydroxyapatite biobased materials for treatment and diagnosis of cancer. *International journal of molecular sciences*, *23*(19), 11352.

[4]. Dorozhkin, S. V., 2015. Calcium orthophosphate-containing biocomposites and hybrid biomaterials for biomedical applications. *Journal of functional biomaterials*, *6*(3), 708-832.

[5]. Radha, G., Manjubaashini, N., & Balakumar, S., 2023. Nano-hydroxyapatite/natural polymer composite scaffolds for bone tissue engineering: a brief review of recent trend. *In vitro models*, *2*(5), 125-151.

[6]. Oni, O. P., Hu, Y., Tang, S., Yan, H., Zeng, H., Wang, H., & Ran, J. 2023. Syntheses and applications of mesoporous hydroxyapatite: a review. *Materials Chemistry Frontiers*, *7*(1), 9-43.

[7]. Ielo, I., Calabrese, G., De Luca, G., & Conoci, S. 2022. Recent advances in hydroxyapatite-based biocomposites for bone tissue regeneration in orthopedics. *International journal of molecular sciences*, *23*(17), 9721.

[8]. Li, L. H., Kim, H. W., Lee, S. H., Kong, Y. M., & Kim, H. E. 2005. Biocompatibility of titanium implants modified by microarc oxidation and hydroxyapatite coating. *Journal of Biomedical Materials Research. Part A 73*(1), 48-54.

[9]. Turon, P., Del Valle, L. J., Alemán, C., & Puiggalí, J., 2017. Biodegradable and biocompatible systems based on hydroxyapatite nanoparticles. *Applied Sciences*, *7*(1), 60.

[10]. Aminzare, M., Eskandari, A., Baroonian, M. H., Berenov, A., Hesabi, Z. R., Taheri, M., & Sadrnezhaad, S. K. 2013. Hydroxyapatite nanocomposites: Synthesis, sintering and mechanical properties. *Ceramics International*, *39*(3), 2197-2206.

[11]. Woodard, J. R., Hilldore, A. J., Lan, S. K., Park, C. J., Morgan, A. W., Eurell, J. A. C., & Johnson, A. J. W. 2007. The mechanical properties and osteoconductivity of hydroxyapatite bone scaffolds with multi-scale porosity. *Biomaterials*, *28*(1), 45-54.

[12]. He, P., Sahoo, S., Ng, K. S., Chen, K., Toh, S. L., & Goh, J. C. H., 2013. Enhanced osteoinductivity and osteoconductivity through hydroxyapatite coating of silk-based tissue-engineered ligament scaffold. *Journal of Biomedical Materials Research part A*, *101*(2), 555-566.

[13]. Shi, H., Zhou, Z., Li, W., Fan, Y., Li, Z., & Wei, J., 2021. Hydroxyapatite based materials for bone tissue engineering: A brief and comprehensive introduction. *Crystals*, *11*(2), 149.

[14]. Kang, S., Haider, A., Gupta, K. C., Kim, H., & Kang, I., 2022. Chemical bonding of

biomolecules to the surface of nano-hydroxyapatite to enhance its bioactivity. *Coatings*, *12*(7), 999.

[15]. Dutta, S. R., Passi, D., Singh, P., & Bhuibhar, A., 2015. Ceramic and non-ceramic hydroxyapatite as a bone graft material: a brief review. *Irish Journal of Medical Science 184(1)*, 101-106.

[16]. Lett, J. A., Sagadevan, S., Fatimah, I., Hoque, M. E., Lokanathan, Y., Léonard, E., & Oh, W. C., 2021. Recent advances in natural polymer-based hydroxyapatite scaffolds: Properties and applications. *European Polymer Journal*, *148*, 110360.

[17]. Sprio, S., Dapporto, M., Preti, L., Mazzoni, E., Iaquinta, M. R., Martini, F., & Tampieri, A., 2020. Enhancement of the biological and mechanical performances of sintered hydroxyapatite by multiple ions doping. *Frontiers in Materials*, *7*, 224.

[18]. Zhao, X., Yang, Z., Liu, Q., Yang, P., Wang, P., Wei, S., & Zhao, Z., 2022. Potential load-bearing bone substitution material: carbon-fiber-reinforced magnesium-doped hydroxyapatite composites with excellent mechanical performance and tailored biological properties. *ACS Biomaterials Science & Engineering*, *8*(2), 921-938.

[19]. Fiume, E., Magnaterra, G., Rahdar, A., Verné, E., & Baino, F. 2021. Hydroxyapatite for biomedical applications: A short overview. *Ceramics*, *4*(4), 542-563.

[20]. Radulescu, D. E., Vasile, O. R., Andronescu, E., & Ficai, A., 2023. Latest research of doped hydroxyapatite for bone tissue engineering. *International Journal of Molecular Sciences*, *24*(17), 13157.

[21]. Du, M., Chen, J., Liu, K., Xing, H., & Song, C., 2021. Recent advances in biomedical engineering of nano-hydroxyapatite including dentistry, cancer treatment and bone repair. *Composites Part B: Engineering*, *215*, 108790.

[22]. Mondal, S., Park, S., Choi, J., Vo, T. M. T., Shin, J. H., Kang, Y. H., & Oh, J., 2020. Rare earth element doped hydroxyapatite luminescent bioceramics contrast agent for enhanced biomedical imaging and therapeutic applications. *Ceramics International*, *46*(18), 29249-29260.

[23]. Gu, M., Li, W., Jiang, L., & Li, X., 2022. Recent progress of rare earth doped hydroxyapatite nanoparticles: Luminescence properties, synthesis and biomedical applications. *Acta Biomaterialia*, *148*, 22-43.

[24]. Somoza, M., Rial, R., Liu, Z., Llovo, I. F., Reis, R. L., Mosqueira, J., & Ruso, J. M., 2023. Microfluidic fabrication of gadolinium-doped hydroxyapatite for theragnostic applications. *Nanomaterials*, *13*(3), 501.

[25]. Uskoković, V., 2015. The role of hydroxyl channel in defining selected physicochemical peculiarities exhibited by hydroxyapatite. *RSC advances*, *5*(46), 36614-36633.

[26]. Mushtaq, A., Zhao, R., Luo, D., Dempsey, E., Wang, X., Iqbal, M. Z., & Kong, X., 2021. Magnetic hydroxyapatite nanocomposites: The advances from synthesis to biomedical applications. *Materials & Design*, *197*, 109269.

[27]. Lv, Y., Shi, Q., Jin, Y., Ren, H., Qin, Y., Wang, B., & Song, S., 2018. Preparation and Luminescent Properties of the antibacterial materials of the La3+ Doped Sm3+-Hydroxyapatite. In *Journal of Physics: Conference Series* 986(1)

[28]. Kim, H. K., Lee, G. H., & Chang, Y., 2018. Gadolinium as an MRI contrast agent. *Future Medicinal Chemistry*, *10*(6), 639-661.

[29]. Fatima, A., Ahmad, M. W., Al Saidi, A. K. A., Choudhury, A., Chang, Y., & Lee, G. H., 2021. Recent advances in gadolinium based contrast agents for bioimaging applications. *Nanomaterials*, *11*(9), 2449.

[30]. Grobner, T., & Prischl, F. C., 2007. Gadolinium and nephrogenic systemic fibrosis. *Kidney international*, *72*(3), 260-264.

[31]. Wei, M., Evans, J. H., Bostrom, T., & Grøndahl, L., 2003. Synthesis and characterization of hydroxyapatite, fluoride-substituted hydroxyapatite and fluorapatite. *Journal of materials science: Materials in medicine*, *14*(4), 311-320.

[32]. Rapacz-Kmita, A., Paluszkiewicz, C., Ślósarczyk, A., & Paszkiewicz, Z., 2005. FTIR and

XRD investigations on the thermal stability of hydroxyapatite during hot pressing and pressureless sintering processes. *Journal of Molecular Structure*, *744*, 653-656.

[33]. Shaltout, A. A., Allam, M. A., & Moharram, M. A., 2011. FTIR spectroscopic, thermal and XRD characterization of hydroxyapatite from new natural sources. *Spectrochimica Acta Part A: Molecular and Biomolecular Spectroscopy*, *83*(1), 56-60.

[34]. Abifarin, J. K., Obada, D. O., Dauda, E. T., & Dodoo-Arhin, D., 2019. Experimental data on the characterization of hydroxyapatite synthesized from biowastes. *Data in brief*, *26*, 104485.

[35]. Zhang, C., Yang, J., Quan, Z., Yang, P., Li, C., Hou, Z., & Lin, J., 2009. Hydroxyapatite nano- and microcrystals with multiform morphologies: controllable synthesis and luminescence properties. *Crystal Growth and Design*, *9*(6), 2725-2733.

[36]. Marković, S., Veselinović, L., Lukić, M. J., Karanović, L., Bračko, I., Ignjatović, N., & Uskoković, D., 2011. Synthetical bone-like and biological hydroxyapatites: a comparative study of crystal structure and morphology. *Biomedical Materials*, *6*(4), 045005.

[37]. Chandrasekar, A., Sagadevan, S., & Dakshnamoorthy, A., 2013. Synthesis and characterization of nano-hydroxyapatite (n-HAP) using the wet chemical technique. *Int. J. Phys. Sci*, 8(32), 1639-1645.

[38]. Montalbano, G., Molino, G., Fiorilli, S., & Vitale-Brovarone, C., 2020. Synthesis and incorporation of rod-like nano-hydroxyapatite into type I collagen matrix: A hybrid formulation for 3D printing of bone scaffolds. *Journal of the European Ceramic Society*, 40(11), 3689-3697.

[39]. Machla, F., Sokolova, V., Platania, V., Prymak, O., Kostka, K., Kruse, B., & Bakopoulou, A., 2023. Tissue engineering at the dentin-pulp interface using human treated dentin scaffolds conditioned with DMP1 or BMP2 plasmid DNA-carrying calcium phosphate nanoparticles. *Acta Biomaterialia*, 159, 156-172.

[40]. Nenad L. Ignjatović, Lidija Mančić, MarinaVuković, Zoran Stojanović, MarkoG. Nikolić, Srečo Škapin, Sonja Jovanović, LjiljanaVeselinović, Vuk Uskoković, Snežana Lazić, Smilja Marković, Miloš M. Lazarević & Dragan P. Uskoković, 2019. Rare-earth (Gd^{3+}, Yb^{3+}/Tm^{3+}, Eu^{3+}) co-doped hydroxyapatite as magnetic, up-conversion and down-conversion materials for multimodal imaging. *Scientific reports, 9:16305*

[41]. James J. Hagan, Susan Cicero Taylor, and Michael F. Tweedle 1988. Fluorescence Detection of Gadolinium Chelates Separated by Reversed-Phase High-Performance Liquid Chromatography, *American Chemical Society, 60, 514-516.*

[42]. Doan, V. H. M., Vu, D. D., Mondal, S., Vo, T. M. T., Ly, C. D., Nguyen, V. T., & Oh, J., 2023. Yb–Gd Codoped Hydroxyapatite as a Potential Contrast Agent for Tumor-Targeted Biomedical Applications. *ACS Biomaterials Science & Engineering*, 9 (8), 4607-4618.

[43]. Minh, D. V. H., 2022. Biomedical instruments design and development focused on ultrasound, fluorescence, and photoacoustic imaging-guided therapeutic modalities, *Doctoral dissertation, 부경대학교.*

[44]. Sha, S., Zhang, L., Liu, H., Chen, J., Che, Y., Zhang, F., & Song, C., 2021. Synthesis and visible-light photocatalytic degradation of Ag 3 PO 4/AgBr/hydroxyapatite ternary nanocomposites prepared from oyster shells. *RSC advances*, 11(26), 15598-15607.

[45]. Kpemissi, M., Eklu-Gadegbeku, K., Veerapur, V. P., Potârniche, A. V., Adi, K., Vijayakumar, S., Banakar, S. M., Thimmaiah, N. V., Metowogo, K., & Aklikokou, K., 2019. Antioxidant and nephroprotection activities of Combretum micranthum: A phytochemical, in-vitro and ex-vivo studies. *Heliyon*, 5(3), e01365.

[46]. Do Amaral, M. B., Viana, R. B., Viana, K. B., Diagone, C. A., Denis, A. B., & de Guzzi Plepis, A. M., 2020. In vitro and in vivo response of composites based on chitosan, hydroxyapatite and collagen. *Acta Scientiarum. Technology,* 42.